

Tunneling between Classically Degenerate Minima: Vortex-Antivortex Oscillations in Trapped Bose Systems

Gentaro Watanabe^{a,b} and C. J. Pethick^a

^a*NORDITA, Blegdamsvej 17, DK-2100 Copenhagen Ø, Denmark*

^b*The Institute of Chemical and Physical Research (RIKEN), 2-1 Hirosawa, Wako, Saitama 351-0198, Japan*

(Dated: January 25, 2020)

The problem of tunneling between classically degenerate minima occurs in a number of different contexts. Here we study the quantum dynamics of a model for a vortex in a Bose gas with repulsive interactions in an anisotropic, harmonic trap. By solving the Schrödinger equation numerically, we show that the circulation of the vortex can undergo periodic reversals by quantum-mechanical tunneling. With increasing interaction strength or particle number, vortices become increasingly stable, and the period for reversals increases. Tunneling between vortex and antivortex states is shown to be described to a good approximation by a Schrödinger cat state that is a superposition of vortex and antivortex states, rather than the mean-field state, and we derive an analytical expression for the oscillation period.

PACS numbers: 03.75.Lm, 05.30.Jp, 67.40.Vs, 03.75.Kk

Mean-field theory is one of the theoretical workhorses in condensed matter physics, nuclear physics, and many other branches of physics. One use of the theory is to estimate tunneling rates, as exemplified by calculations of the decay of superflow in liquid helium [1], alpha decay of nuclei [2], and collapse of Bose-Einstein condensed atomic clouds with attractive interactions [3]. It is therefore of importance to examine models which can be solved without invoking the mean-field approximation. The model we consider in this paper is relevant to at least two different situations in the physics of ultracold atomic Bose gases. One occurs in connection with the dynamics of vortices, which has been explored extensively in recent years [4]. The other is tunneling of atoms with attractive interactions between the minima of a double-well potential [5]. For definiteness, we shall use the language of the former problem, but the mathematics of the two problems is essentially identical.

An interesting prediction by García-Ripoll *et al.* [6] within the mean-field approach is that a rotating Bose-Einstein condensate in a non-rotating anisotropic harmonic trap can undergo periodic reversals of the sign of the vorticity if the initial energy of the system is sufficient to overcome the energy barrier between vortex states with opposite circulation. In this paper we consider the problem quantum-mechanically, and show by solving the Schrödinger equation numerically that for energies below the barrier, reversals of the vorticity can occur by tunneling. We find that the wave function during reversals resembles more closely a Schrödinger cat state than a mean-field one, and we derive an analytical expression for the rate of reversals that agrees well with the numerical data.

Consider N identical bosons of mass m in an anisotropic, harmonic two-dimensional trap, with trap frequencies denoted by ω_x and ω_y , and for definiteness we shall assume that $\omega_x > \omega_y$. Following Ref. [6] we shall as-

sume that the only oscillator levels occupied are the first excited states of the oscillators [7], corresponding to the wave functions $\psi_x \equiv C (x/d_x) \exp(-x^2/2d_x^2 - y^2/2d_y^2)$, where $C = \sqrt{2/(\pi d_x d_y)}$ and $d_x \equiv \sqrt{\hbar/m\omega_x}$ and a similar expression for ψ_y . The many-body Hamiltonian is

$$H = H_0 + H_{\text{int}} = \sum_{i=x,y} \epsilon_i \hat{c}_i^\dagger \hat{c}_i + \frac{1}{2} \sum_{i,j,k,l=x,y} \langle ij | V | kl \rangle \hat{c}_i^\dagger \hat{c}_j^\dagger \hat{c}_l \hat{c}_k, \quad (1)$$

with $\epsilon_i \equiv \hbar\bar{\omega} + \hbar\omega_i$ ($i = x, y$), where \hat{c}_i^\dagger creates and \hat{c}_i destroys a particle in the state ψ_i . We shall take the interaction to have the contact form $\langle \mathbf{r}, \mathbf{r}' | V | \mathbf{r}, \mathbf{r}' \rangle = g_{2D} \delta^2(\mathbf{r} - \mathbf{r}')$, where g_{2D} is an effective two-dimensional interaction strength, which we shall take to be positive [8].

For orientation we first describe the mean-field approach [for this case the Gross-Pitaevskii (GP) approximation], in which one assumes that all particles are in the same single-particle state. Thus the many-body state may be written as

$$|\Delta\phi, \Delta n\rangle \equiv \frac{1}{\sqrt{N!}} \left(n_x^{1/2} \hat{c}_x^\dagger + n_y^{1/2} \hat{c}_y^\dagger e^{-i\Delta\phi} \right)^N |0\rangle. \quad (2)$$

The quantities n_x and n_y are the occupation probabilities of the two states, and $n_x + n_y = 1$ and $\Delta n \equiv n_x - n_y$. The phase difference between the two components is denoted by $\Delta\phi \equiv \phi_x - \phi_y$, where ϕ_x and ϕ_y are the phases of the two states, and $|0\rangle$ is the vacuum state. The GP energy functional is [9]

$$\frac{E}{N} = \int d^2r \left\{ \frac{\hbar^2}{2m} |\nabla\psi|^2 + \frac{m}{2} (\omega_x^2 x^2 + \omega_y^2 y^2) |\psi|^2 + \frac{g_{2D}}{2} |\psi|^4 \right\}, \quad (3)$$

where ψ is the condensate wave function, $\psi = a_x \psi_x + a_y \psi_y = |a_x| e^{i\phi_x} \psi_x + |a_y| e^{i\phi_y} \psi_y$ with $|a_x|^2 + |a_y|^2 = N$.

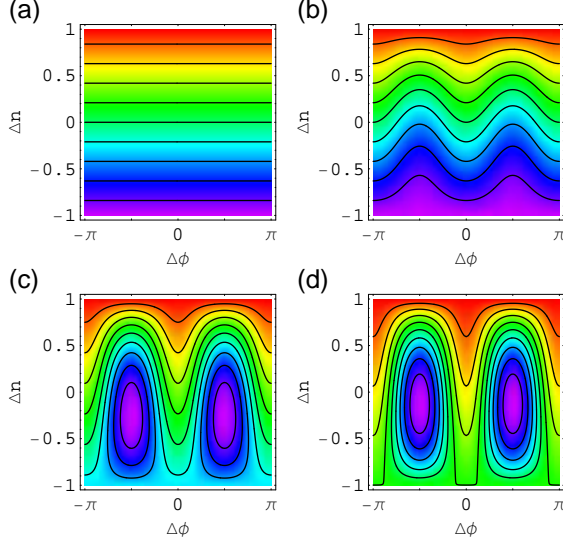


FIG. 1: (Color online) Landscape of the energy per particle \mathcal{E} for $\Gamma = 0$ (a), 0.8 (b), 4.0 (c), and 8.0 (d). Purple regions (the darker area for $\Delta n \lesssim 0$) correspond to lower \mathcal{E} and red ones (the darker area for $\Delta n \simeq 1$) to higher \mathcal{E} . For a given panel, the contour lines are equally spaced in \mathcal{E} , but the spacing varies from panel to panel.

Evaluation of Eq. (3) for this wave function leads to

$$\mathcal{E} \equiv \frac{E}{\hbar\bar{\omega}N} = \frac{1}{2} \frac{\Delta\omega}{\bar{\omega}} \Delta n - \frac{\gamma}{4} [1 - (\Delta n)^2] \sin^2 \Delta\phi, \quad (4)$$

where $\gamma \equiv \gamma_0 \sqrt{\omega_x \omega_y / \bar{\omega}^2}$, with $\gamma_0 \equiv N a_s / Z$, and $\bar{\omega} \equiv (\omega_x + \omega_y) / 2$. In Eq. (4) we have omitted the contribution independent of Δn and $\Delta\phi$ [10]. One sees that there is one dimensionless parameter in the problem, $\Gamma \equiv \gamma\bar{\omega} / \Delta\omega$.

In Fig. 1, we show contours of \mathcal{E} as a function of $\Delta\phi$ and Δn for several values of the interaction strength. States with $\Delta\phi = -\pi/2$ are vortex-like with positive circulation, while those with $\Delta\phi = \pi/2$ correspond to an antivortex, a vortex with negative circulation. States with $\Delta\phi = 0, \pi$ have nodal lines which, because of the larger mean square density, give rise to larger repulsive energy. Allowed motions correspond to contours of constant energy. For small Γ [Fig. 1(a) and (b)], all contours are open, and the allowed motions correspond to oscillations between vortex states and antivortex ones. For $\Gamma > 1$, global minima of the energy develop on the lines $\Delta\phi = -\pi/2$ and $\pi/2$, and there are closed contours surrounding the minima. These correspond to motions in which a vortex line oscillates without reversals of the circulation. With further increase of Γ , the closed contours occupy an increasing fraction of the area [see Fig. 1(c) and (d)] and an energy barrier with height $\sim \gamma\hbar\bar{\omega} \sim \hbar\bar{\omega}N a_s / Z$ per particle grows between the vortex and antivortex states, i.e., large Γ stabilizes the vortex and antivortex states. Classically, for a system having energy less than the minimum value

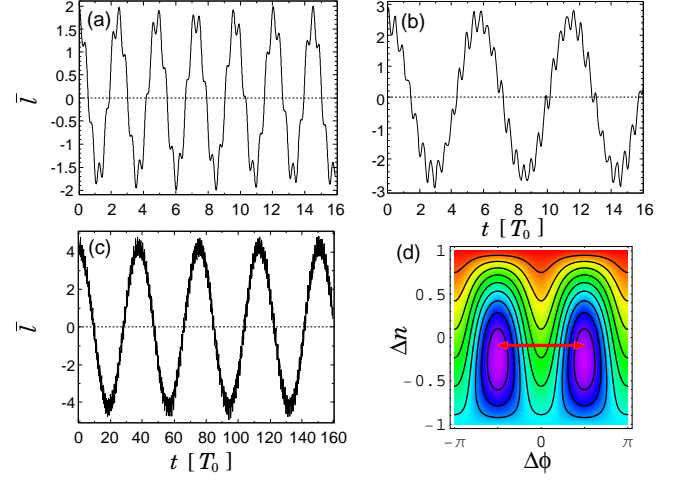


FIG. 2: (Color online) Time evolution of \bar{L} for $\Gamma = 4.0$ and $N = 2$ (a), 3 (b), and 5 (c).

on the line $\Delta\phi = 0$, the circulation of a vortex cannot change sign.

However, in quantum mechanics the circulation can reverse by tunneling, as we now show. The interaction Hamiltonian is given by $H_{\text{int}} = (\gamma\hbar\bar{\omega}/4N)h_{\text{int}}$ with

$$\begin{aligned} h_{\text{int}} = & \hat{c}_x^\dagger \hat{c}_x^\dagger \hat{c}_y \hat{c}_y + \hat{c}_y^\dagger \hat{c}_y^\dagger \hat{c}_x \hat{c}_x + 4\hat{c}_x^\dagger \hat{c}_y^\dagger \hat{c}_y \hat{c}_x \\ & + 3(\hat{c}_x^\dagger \hat{c}_x^\dagger \hat{c}_x \hat{c}_x + \hat{c}_y^\dagger \hat{c}_y^\dagger \hat{c}_y \hat{c}_y) \\ = & 3\hat{N}^2 - 2\hat{N} - \hat{l}^2. \end{aligned} \quad (5)$$

Here $\hat{N} \equiv \hat{c}_x^\dagger \hat{c}_x + \hat{c}_y^\dagger \hat{c}_y$ is the total number operator and $\hat{l} \equiv i(\hat{c}_y^\dagger \hat{c}_x - \hat{c}_x^\dagger \hat{c}_y)$. The expectation value L of the z -component of the angular momentum operator in a state $|\Psi\rangle$ containing only the two single-particle states ψ_x and ψ_y is given by $L = \hbar\sqrt{\bar{\omega}^2 / \omega_x \omega_y} \langle \Psi | \hat{l} | \Psi \rangle \equiv \hbar\sqrt{\bar{\omega}^2 / \omega_x \omega_y} \bar{l}$. The system has $N + 1$ Fock states $|N_x, N_y\rangle = |N_x, N - N_x\rangle$ with $N_x = 0, 1, \dots, N$, where N_x and N_y are the numbers of particles occupying the single particle states ψ_x and ψ_y , respectively. Using the above many-body Hamiltonian, we have followed the time evolution of the system, starting from the vortex state $\propto (\hat{c}_x^\dagger + i\hat{c}_y^\dagger)^N |0\rangle$, corresponding to $|-\pi/2, 0\rangle$ for the particular choice $\Delta\omega/\bar{\omega} = 0.01$. Preliminary results were reported in Ref. [11].

Classically, reversals of the circulation with this initial state are impossible if $\Gamma > 2$, which ensures that the state lies on a closed orbit. However, we see, e.g., in Fig. 2 for $\Gamma = 4.0$, that reversals of the angular momentum do occur. The angular momentum oscillates with a period $T \simeq 2.41 T_0$ for $N = 2$, $T \simeq 5.73 T_0$ for $N = 3$, and $T \simeq 37.7 T_0$ for $N = 5$, where $T_0 = 2\pi/\Delta\omega$ is the period in the absence of interactions. The rapid wiggles in Fig. 2(a)-(c) are due to oscillations of internal degrees of freedom of the vortex, which correspond to motion on closed energy contours in the mean-field approach.

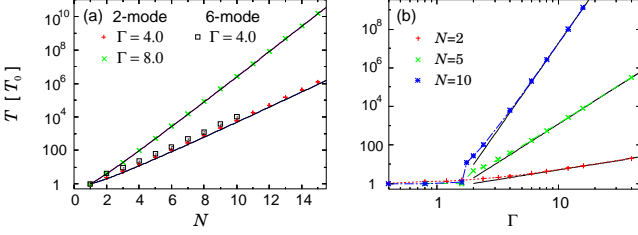


FIG. 3: (Color online) Tunneling period T as a function of N at fixed interaction strength Γ [panel (a)] and as a function of Γ at fixed N [panel (b)]. The thick solid lines for $\Gamma \geq 2$ are calculated from an analytic formula (7). The lines connecting the data points in panel (b) are to guide the eye. The period T for the data points at $\Gamma = 1.6$ in panel (b) is hard to define and has an uncertainty of order $0.1 T_0$.

In Fig. 3(a), we plot the oscillation period T as a function of N for $\Gamma = 4.0$ and 8.0 . The results do not change qualitatively for a more general model in which six single-particle states, the ground state and the three lowest d -like states in addition to the two p -like states, are taken into account. We see clearly that T increases almost exponentially with N . This tendency is consistent with the fact that, for these values of Γ , the vortex and antivortex states are stable classically. We also see that T increases with Γ . This is because for $\Gamma \gg 1$ the Hamiltonian is dominated by H_{int} and therefore level spacings are proportional to γ . Thus mixing of states by the anisotropy becomes less important for large Γ . For $\Gamma < 1$, the oscillation period is approximately T_0 , as one would expect from the fact that under these conditions reversals can occur in classical mean-field theory for all initial conditions. For $\Gamma \ll 1$, we see repetitive collapses and revivals of L with a period $\sim 2\pi N/\gamma\bar{\omega}$ [12].

In Fig. 3(b), we plot T as a function of Γ for fixed N . We can see the different behaviors for $\Gamma \lesssim 1$ and $\Gamma \gtrsim 1$. The oscillations in the former region are well described by mean-field theory and T is almost constant with a value $\sim T_0$. For large Γ , vortex-antivortex oscillation occurs for the given initial conditions only in the quantum-mechanical calculation, and T shows a power-law dependence on Γ .

To understand the behavior of the tunneling time, we have investigated the state $|\Psi(t)\rangle$. Figure 4 shows its overlap $|\langle\Psi|\Delta\phi_{\text{opt}}, 0\rangle|$ with the mean-field state (2), where $\Delta\phi_{\text{opt}}$ is chosen to maximize the overlap. Expectation values of \hat{l} , which are proportional to those of the angular momentum, are also plotted, and they are denoted by \bar{l} for $|\Psi(t)\rangle$ and \bar{l}_{opt} for $|\Delta\phi_{\text{opt}}, 0\rangle$. For $\Gamma \lesssim 1$, $|\Psi(t)\rangle$ is well described by the mean-field state, and $\Delta\phi_{\text{opt}}$ changes continuously. For $\Gamma_0 = 2.4$ and 8.0 , $\Delta\phi_{\text{opt}}$ jumps essentially discontinuously between approximately $-\pi/2$ and $\pi/2$, corresponding to the vortex and antivortex states. This indicates that the main components of the state correspond to either all particles being

in the vortex state or all of them in the antivortex state, and components in which some particles are in the vortex state and others in the antivortex state are suppressed. A much better approximation for the wave function for $\Gamma \gg 1$ is the Schrödinger cat state consisting of a superposition of the states in which all particles are in the vortex state or all particles are in the antivortex state,

$$|\text{Cat}; \theta\rangle \equiv \cos \frac{\theta}{2} \left| -\frac{\pi}{2}, 0 \right\rangle + i \sin \frac{\theta}{2} \left| \frac{\pi}{2}, 0 \right\rangle. \quad (6)$$

In Fig. 5, we plot the overlap $|\langle\Psi|\text{Cat}; \theta_{\text{opt}}\rangle|$ for the same $|\Psi\rangle$ as in Fig. 4(d). Similarly, θ_{opt} is determined by maximizing $|\langle\Psi|\text{Cat}; \theta_{\text{opt}}\rangle|$. Here L_{opt} is the expectation value of the angular momentum in the state $|\text{Cat}; \theta_{\text{opt}}\rangle$. It is remarkable that θ_{opt} changes almost continuously and the overlap is close to unity (its mean value is $\simeq 0.97$ for this case).

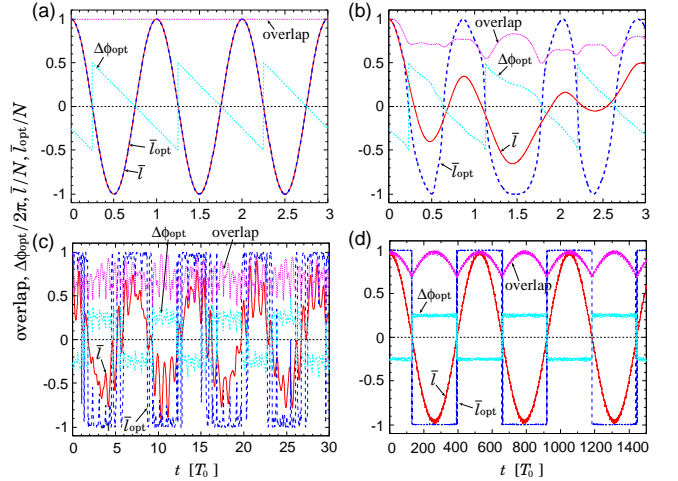


FIG. 4: (Color online) Overlap $|\langle\Psi|\Delta\phi_{\text{opt}}, 0\rangle|$ of the wave function with the optimized phase state for $N = 5$ and $\Gamma = 0$ (a), 1.6 (b), 2.4 (c), and 8.0 (d).

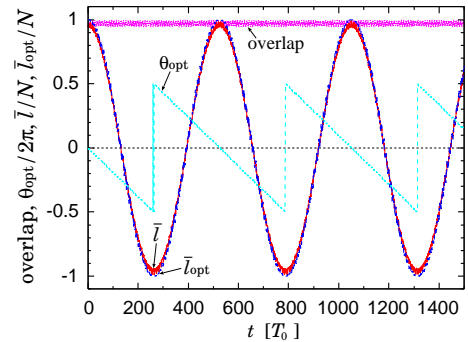


FIG. 5: (Color online) Overlap $|\langle\Psi|\text{Cat}; \theta_{\text{opt}}\rangle|$ of the numerical solution of the wave function with the cat state for $N = 5$ and $\Gamma = 8.0$.

The behavior of the wave function for $\Gamma \gg 1$ is most conveniently analysed in terms of

states in which the interaction energy is diagonal. These may be written as $|l\rangle = \{[(N+l)/2]![(N-l)/2]!\}^{-1/2} (c_+^\dagger)^{(N+l)/2} (c_-^\dagger)^{(N-l)/2} |0\rangle$, where the operators $\hat{c}_+^\dagger \equiv (\hat{c}_x^\dagger + i\hat{c}_y^\dagger)/\sqrt{2}$ and $\hat{c}_-^\dagger \equiv (\hat{c}_x^\dagger - i\hat{c}_y^\dagger)/\sqrt{2}$ create particles in a vortex or an antivortex state, respectively. The operator \hat{l} in the subspace of states we are considering is $\hat{c}_+^\dagger \hat{c}_+ - \hat{c}_-^\dagger \hat{c}_-$. The anisotropy of the trap couples states of different l according to the Hamiltonian $H' = (\hbar\Delta\omega/2)(\hat{c}_+^\dagger \hat{c}_- + \hat{c}_-^\dagger \hat{c}_+)$. The wave function is dominated by the vortex and antivortex states, and components from other states are suppressed by the large interaction energy for these states. The physics is analogous to that for tunneling of particles with attractive interactions in a double-well potential [5]. Because of the anisotropy, the vortex and antivortex states are not energy eigenstates and the leading contributions to the mixing of the states for large Γ may be calculated by perturbation theory. Since the anisotropy couples only states in which l differs by 2, it is of N th order in $\Delta\omega$. The leading contribution to the matrix element mixing the vortex and antivortex states is $\Delta E = 2H'_{-N,-N+2}(\Delta E_{-N+2})^{-1} \cdots H'_{N-4,N-2}(\Delta E_{N-2})^{-1} H'_{N-2,N}$, where $H'_{l,l+2} = \langle l|H'|l+2\rangle$ and $\Delta E_l = E_l - E_N$, with $E_l = -(\gamma\hbar\bar{\omega}/4N)l^2$. Therefore the splitting of the two lowest states for $\Gamma \gg 1$ is

$$\Delta E = \hbar|\Delta\omega|N \left(\frac{\alpha(N)}{\Gamma} \right)^{N-1}. \quad (7)$$

Here $\alpha(N) \equiv N[(N-1)!]^{-1/(N-1)}/2$ is a function that depends weakly on N : $\alpha(2) = 1$ and $\alpha(\infty) = e/2$. The tunneling period is given by $T = 2\pi\hbar/\Delta E$. In the strong interaction regime, ΔE given by Eq. (7) accounts very well for the numerical results, as is shown in Fig. 3. We remark that rotation will suppress the vortex-antivortex oscillations if $2N\hbar\Omega \gtrsim \Delta E$, where Ω is the rotational angular velocity.

In conclusion, we have calculated tunneling rates without making a mean-field approximation and have obtained an analytical result in the limit of small tunneling. Our results provide a useful benchmark for determining the accuracy of semiclassical approaches based on mean-field theory. We have demonstrated that the wave function is much better described as a Schrödinger cat state, which for the present problem is a superposition of a

state in which all particles are in the vortex state and one in which all particles are in the antivortex state. On the experimental side, recent advances in creating few-body systems trapped on an optical lattice [13, 14] offer the possibility of observing experimentally the effects we predict.

The authors are grateful to Jason Ho and Jacobus Verbaarschot for valuable discussions and Eugene Zaremba for helpful comments. This work was supported by the JSPS.

- [1] J. S. Langer and M. E. Fisher, *Phys. Rev. Lett.* **19**, 560 (1967).
- [2] See, A. Bohr and B. Mottelson, *Nuclear Structure* (Benjamin, New York, 1975) Vol. II, Ch.6.
- [3] M. Ueda and A. J. Leggett, *Phys. Rev. Lett.* **80**, 1576 (1998).
- [4] A. L. Fetter and A. A. Svidzinsky, *J. Phys.: Condens. Matter* **13**, R135 (2001); G. Baym, *J. Low Temp. Phys.* **138**, 601 (2005).
- [5] T.-L. Ho and C. V. Ciobanu, *J. Low Temp. Phys.* **135**, 257 (2004).
- [6] J. J. García-Ripoll, G. Molina-Terriza, V. M. Pérez-García, and L. Torner, *Phys. Rev. Lett.* **87**, 140403 (2001).
- [7] This situation could be realized in practice by, e.g., making the trap anharmonic, thereby lifting degeneracies present for a harmonic potential.
- [8] For a system uniform in the z direction, and with the usual Gross-Pitaevskii assumption, $g_{2D} = g/Z$, where Z is the extent of the cloud in the z direction, $g \equiv 4\pi\hbar^2 a_s/m$ is the two-body interaction strength in three dimensions, and a_s is the s -wave scattering length.
- [9] We have here made the usual replacement of $1 - 1/N$ by unity. This does not affect our conclusions.
- [10] Reference [6] considered the case $\sin^2\Delta\phi = 1$, and our Eq. (4) then agrees with Eq. (6) of that paper.
- [11] G. Watanabe, in the proceedings of LPHYS06, *Laser Phys.* **17**, 533 (2007).
- [12] This can be understood from the fact that the contribution to the level spacing of the Fock states from the \hat{l}^2 term in h_{int} is $\langle N_x, N_y | \hat{l}^2 | N_x, N_y \rangle = N + [N^2 - (N_x - N_y)^2]/2$, and thus the situation is essentially the same as that considered by A. Imamoglu, M. Lewenstein, and L. You, *Phys. Rev. Lett.* **78**, 2511 (1997) and L. P. Pitaevskii, *Phys. Lett. A* **229**, 406 (1997).
- [13] G. K. Campbell *et al.*, *Science* **313**, 649 (2006).
- [14] S. Fölling *et al.*, *Phys. Rev. Lett.* **97**, 060403 (2006).